SF2A 2021
A. Siebert, K. Baillié, E. Lagadec, N. Lagarde, J. Malzac, J.-B. Marquette, M. N'Diaye, J. Richard, O. Venot (eds)

OBSERVATIONAL APPEARANCE OF CIRCUMBINARY DISCS

K. Hirsh[1] and J.-F. Gonzalez[1]

Abstract. Binary companions are known to open large cavities in their circumbinary discs. Resolving a binary companion, however, remains a difficult observational problem and there exists a number of discs with observed cavities and as yet no resolved binary. An indirect detection method is therefore needed to infer the presence of a binary companion in these systems. As such we investigate the effect of a binary companion on the circumbinary disc in an attempt to find some signatures detectable in observations. We perform radiative transfer calculations on a suite of SPH simulations to create synthetic observations. We investigate the signal in the moment 1 and CO channel maps and develop a metric which aids in the inference of an otherwise undetected binary companion.

Keywords: accretion discs - binaries - radiative transfer - methods: numerical

1 Introduction

In Hirsh et al. (2020) we simulated a suite of circumbinary discs using the Smoothed Particle Hydrodynamics code `PHANTOM` (Price et al. 2018) in order to investigate the effects of the binary and disc properties on the cavity size. The reverse problem of inferring the presence of a binary companion from observations of a cavity also remains an open question, since there exists many systems displaying large cavities with no detected binary as yet (e.g: van der Marel et al. 2016; Canovas et al. 2018; Ubeira Gabellini et al. 2019). To this end we use the radiative transfer code `MCFOST` (Pinte et al. 2006, 2009) to compute synthetic moment 1 maps, as well as synthetic channel maps, of the simulated discs in Hirsh et al. (2020). We then examine these synthetic images to better understand how the presence a binary companion can be inferred from observations and we develop a metric to quantify the effect the binary has on the disc.

2 Definition of Asymmetry Metric

We define an metric to quantify the asymmetry in the disc. This is done by measuring the asymmetry in two opposite velocity CO channels by flipping the positive channel across the y-axis and subtracting from the negative channel (note that the choice of which branch to flip is arbitrary). The resulting images are show in Figure 1). We then define the asymmetry in the channel as the L2 norm of the flux in the subtracted image, normalised to the integrated flux in the positive channel. This is given by:

$$\aleph_c = \frac{\sqrt{\sum_{i,j} \Delta F_{ij}^2}}{F}, \tag{2.1}$$

where $\aleph_c$ is the asymmetry in channel c, ΔF_{ij} is the flux on pixel (i, j) in the subtracted image and F is the integrated flux. Normalising to the integrated flux gives a non-dimensional $\aleph_c$ that is insensitive to field of view and signal strength.

Figure 2 gives $\aleph_c$ for a disc with binary mass ratio $q = 0.1$, aspect ratio $H/R_{\rm in} = 0.05$, coplanar disc ($i = 0°$), and a number of binary eccentricities are shown. A local maximum is seen near the 0 velocity channel and have an increasing $\aleph_c$ at high velocity channels. Since $\aleph_c$ has only small variations in each channel we are free to take the average over all visible channels to get $\aleph$, the total disc asymmetry. This allows us to quantify the disc as a whole and has the advantage of allowing us to compare two discs even if part of one disc is obscured by removing the obscured channels from the average.

[1] Univ Lyon, Univ Claude Bernard Lyon 1, ENS de Lyon, CNRS, Centre de Recherche Astrophysique de Lyon UMR5574, F-69230, Saint-Genis-Laval, France

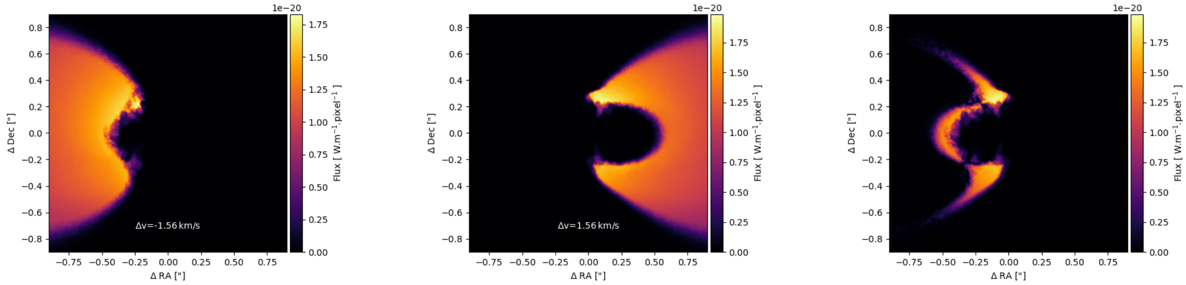

Fig. 1: Left and Middle: 2 channel maps with opposite velocities. Right: Flux differential between the two channels, the positive branch has been flipped horizontally and subtracted from the negative branch. Here the absolute value of the difference has been plotted to give $F_{\rm min} = 0$.

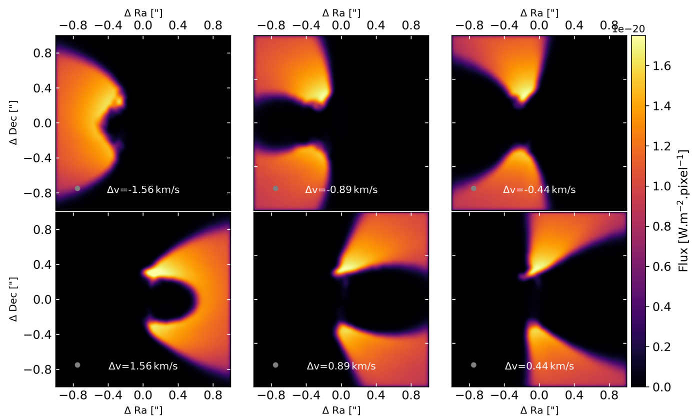

Fig. 3: A selection of CO channel maps of a coplanar disc with $(H/R)_{\rm in} = 0.05$, surrounding a binary with $q = 0.1$, with an angle of 22.5° on the plane of the sky, after 1000 binary orbits. The top row shows only the negative branch and the bottom row shows the corresponding channels in the positive branch, highlighting the asymmetry in the disc.

2.1 *Binary Eccentricity*

Figure 3 shows a selection of CO channel maps for the disc in Figure 1. Large asymmetries are visible in opposite channels. We calculate $\aleph$ for this disc, as well as a suite of discs with increasing eccentricity up to $e = 0.9$, and for a single star disc with the same properties. The variation of $\aleph$ with eccentricity is shown in Figure 4, plotted with the single star disc for comparison. From this we can see that, with the exception of a circular binary, disc around binaries with $e > 0.4$ are more asymmetric than those around binaries with $e < 0.4$. Furthermore, even the least asymmetric circumbinary discs are roughly 3 times more asymmetric than a single star disc.

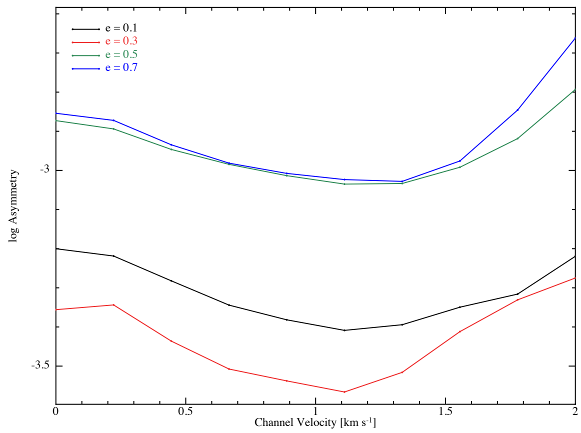

Fig. 2: Asymmetry metric $\aleph_c$ as a function of channel velocity.

2.2 *Disc Scale Height*

Figure 5 shows the dependence of $\aleph$ on disc scale height, with less viscous discs being more asymmetric. This is to be expected as viscosity acts to shrink and circularise the cavity (e.g: Artymowicz & Lubow 1994; Hirsh et al. 2020), thereby decreasing $\aleph$. This counteracts the dynamical effects from the binary which act to open a large, eccentric cavity, thereby increasing $\aleph$.

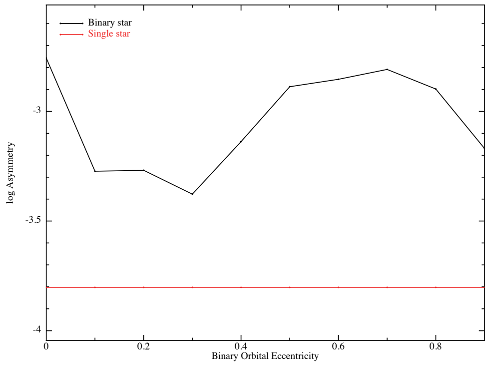

Fig. 4: Black line: Asymmetry as a function of binary orbital eccentricity for a coplanar disc with $(H/R)_{\rm in} = 0.05$ surrounding a binary with $q = 0.1$ after 1000 binary orbits. Red line: Asymmetry of a single star disc with the same properties. Note that binary orbital eccentricity has no meaning for a single star disc, and this disc is only plotted as a horizontal line for ease of comparison with the suite of circumbinary discs.

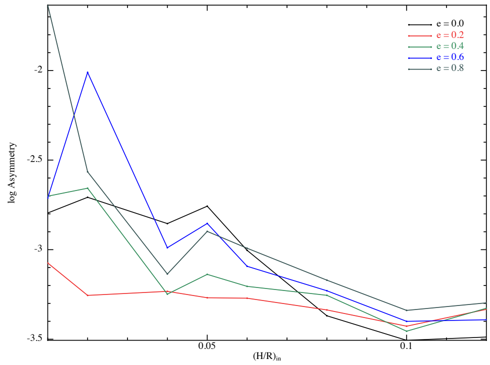

Fig. 5: Asymmetry as a function of disc aspect ratio for coplanar discs surrounding a binary with q = 0.1 after 1000 binary orbits. Different lines depict discs with different binary orbital eccentricities.

3 Moment 1 Maps

The top left panel of Figure 6 gives the moment 1 map for the disc described in Section 2, which shows the line of sight velocity of the material in the disc. Examining the $v = 0$ iso-velocity line, that is the line of the material which has no line of sight velocity, we see a twist inside the cavity. To investigate this peculiar shape we consider the effects of the radial and azimuthal components of the gas velocity in the plane of disc. We remove the radial component of the velocity by setting the $v_r = 0$ in the final output of the `PHANTOM` simulation before recomputing the moment 1 map with `MCFOST`. We then repeat this procedure, but keep the original v_r and instead set $v_\phi = v_{\rm k}$, that is the azimuthal velocity is that of a Keplerian orbit. Finally, we force the velocity to be fully Keplerian, that is $v_r = 0$ and $v_\phi = v_{\rm k}$. The effect of changing the radial and azimuthal velocity of the gas on the moment 1 map are also shown in Figure 6. When we remove the radial component of the velocity of the gas (top-right panel) this asymmetry largely vanishes, with the $v = 0$ line becoming much straighter. When we set the material to orbit with a Keplerian v_ϕ (bottom-left panel) the asymmetry remains. Finally, if we set the material on a purely Keplerian orbit (bottom-right panel) the shape resembles that of the observation with the radial velocity removed. This shows that the asymmetric shape of the moment 1 map is caused by the radial velocity of the material in the disc, while the deviations from Keplerian motion in the azimuthal direction have only a minor effect on the shape of the moment 1 map. The two most obvious sources of radial motion are binary-disc interactions and viscous accretion. Figure 7 compares the moment 1 maps of the fiducial disc with that of a disc with the same properties, but surrounding a single star. In the single star case the only source of radial motion is viscous accretion, and this is not strong enough to produce a twist in the moment 1 map. Therefore the source of the twist in the moment 1 maps of our discs is the companion.

4 Discussion

In defining ℵ, and while discussing the physical features present in the discs, we frequently refer to the positive and negative branches of the channel maps. It is important to stress that discussing these branches are unique to each individual disc. This is because which half of the disc appears in which branch is dependant on both the phase of the orbit and the position of the observer. For example, if the observer was positioned on the other side of the disc the positive and negative branches would be swapped. Therefore we caution the reader that a feature we see in, e.g., the positive branch is not constrained to only ever appear in the positive branch for all discs.

In this work we only investigated the dependence of ℵ on binary orbital eccentricity and disc scale height.

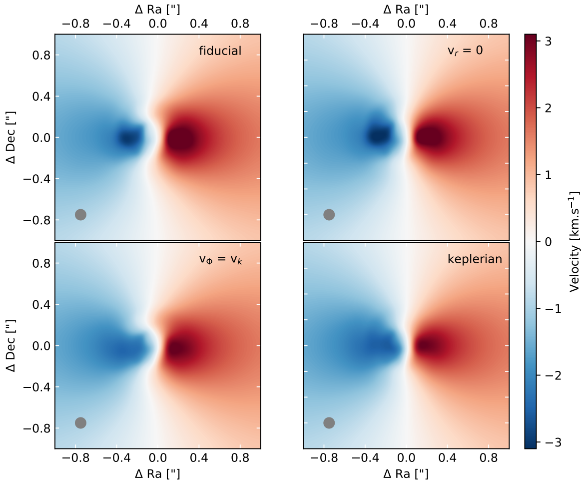

Fig. 6: Top left panel: Moment 1 map of a coplanar disc with $(H/R)_{\rm in} = 0.05$ surrounding a binary with $q = 0.1$, oriented with an inclination of 22.5° on the plane of the sky. Top right panel: Same, but with forcing $v_r = 0$. Bottom left panel: Same as top left, but with forcing $v_\phi = v_k$. Bottom right: Same as top left, but with forcing a fully Keplerian velocity.

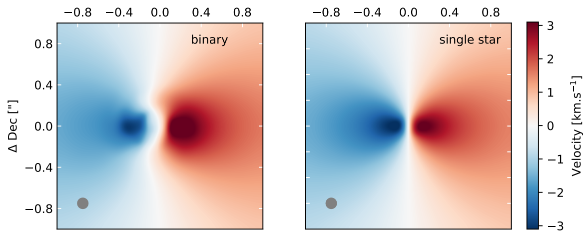

Fig. 7: Left panel: Moment 1 map of a coplanar disc with $(H/R)_{\rm in} = 0.05$ surrounding a binary with $q = 0.1$, oriented with an inclination of 22.5° on the plane of the sky (top left panel from Fig 6). Right panel: Moment 1 map of a disc with the same properties, but surrounding a single star.

In future work we will calculate ℵ for all discs simulated in Hirsh et al. (2020), to investigate the dependence on binary-disc inclination and binary mass ratio. Beyond that performing this analysis on real observation, rather than the synthetic observations presented here, would allow us to test its validity in inferring the presence of a binary companion. Once confirmed this could be applied to transitional discs without a known companion to infer whether or not one is there.

5 Conclusion

We have generated a suite of synthetic observations of circumbinary discs, examining them to find signatures of the binary in these observations. We have also developed a metric to quantify the asymmetry, ℵ, in the channel maps and applied it to our synthetic CO channel maps. We found that the radial motion of the gas caused by binary-disc interactions leads to a twist in the moment 1 maps. Furthermore, single star discs have an asymmetry of $\log(\aleph) \sim -3.8$. The most symmetric circumbinary discs have a large scale height and low binary eccentricity. In these cases we find $\log(\aleph) \sim -3.5$. Conversely, thin discs around highly eccentric binaries can have asymmetries of $\log(\aleph) \sim -2$. It is important to note, however, that while a twisted moment 1 map, or an asymmetry of $\log(\aleph) \gtrsim -3.5$, do not constitute detections of a stellar companion, they do strongly hint towards their presence. As such, they can be used to identify systems that would make a good candidate for deeper observations with the intent of detecting a stellar companion.

References

Artymowicz, P. & Lubow, S. H. 1994, ApJ, 421, 651
Canovas, H., Montesinos, B., Schreiber, M. R., et al. 2018, A&A, 610, A13
Hirsh, K., Price, D. J., Gonzalez, J.-F., Ubeira-Gabellini, M. G., & Ragusa, E. 2020, MNRAS, 498, 2936
Pinte, C., Harries, T. J., Min, M., et al. 2009, A&A, 498, 967
Pinte, C., Ménard, F., Duchêne, G., & Bastien, P. 2006, A&A, 459, 797
Price, D. J., Wurster, J., Tricco, T. S., et al. 2018, PASA, 35, e031
Ubeira Gabellini, M. G., Miotello, A., Facchini, S., et al. 2019, MNRAS, 486, 4638
van der Marel, N., van Dishoeck, E. F., Bruderer, S., et al. 2016, A&A, 585, A58